AJNR Am J Neuroradiol 25:108–111, January 2004

Effect of Region of Interest on Interobserver Variance in Apparent Diffusion Coefficient Measures

Yasemin Bilgili and Birsen Unal

BACKGROUND AND PURPOSE: **Apparent diffusion coefficient (ADC) values derived from diffusion-weighted MR imaging are useful measurements for assessment of cellular alterations in pathologic conditions of the brain. In this study, two radiologists independently quantitated ADCs and region-of interest sizes in prespecified locations of human brain to test interobserver ADC variance and the effect of varying ROI sizes on ADC differences.**

METHODS: **Twenty-seven patients with normal MR findings underwent diffusion-weighted imaging (b value = 1000 s/mm^2) on a 1.5-T system. Two radiologists independently placed two ROI areas of 22 ± 5 mm^2 and 62 ± 6 mm^2 (former area inside the latter area) at different sites of the brain (centrum semiovale, frontal white matter, nucleus caudatus, putamen, thalamus, substantia nigra, red nucleus, and pons) from trace images. Differences in ADC measurement obtained from each region of the brain for each radiologist and the size of each ROI were compared statistically.**

RESULTS: **Mean ADC of prespecified areas of brain ranged between 0.673 and 0.818 mm^2/s $\times 10^{-3}$. Interobserver variance was significant in some of the specified areas (centrum semiovale, frontal white matter, pons, substantia nigra, and red nucleus). Varying ROI sizes at the pons, substantia nigra, and red nucleus yielded statistically different ADC values.**

CONCLUSION: **ADC values are found to be unreliable for use in assessing brain disease in some specified areas of the brain owing to interobserver variance and different ROI sizes.**

MR imaging has excelled at depicting macroscopic anatomy of the human brain; however, many normal cellular functions and disease processes, such as early acute cerebral ischemia, that occur at the microscopic level do not affect conventional MR relaxation parameters and are poorly assessed with conventional MR imaging (1). In this study, interobserver variability and effects of different-sized regions of interest (ROI) on ADC values were investigated.

Methods

Twenty-seven patients in whom cranial MR examinations were judged normal were selected for study. Two radiologists (Y.B., B.U.) independently determined that T1- and T2-weighted findings were normal in all subjects; no one had more than three very small (<3 mm in diameter) areas of hyperintensity on T2-weighted images in the brain parenchyma.

Received April 10, 2003; accepted after revision July 22.

Presented at the 2003 European Congress of Radiology, March 7–11, Vienna, Austria.

From the Department of Radiology, Kirikkale University School of Medicine, Süleyman Demirel Hospital, Kirikkale, Turkey.

Address correspondence to Dr. M. Yasemin K. Bilgili, Sevil sokak 16/3 06590, Cebeci Ankara, Turkey.

All experiments were performed by using a head coil in conduction with a 1.5-T whole-body imager (Infinion; Philips Medical Systems, Cleveland, OH) with a maximum gradient amplitude of 50 mT/m and a maximum gradient slew rate of 100 mT/m/s. The head coil had an inner diameter of 27 cm.

Before diffusion-weighted MR imaging, T1-weighted images were acquired in the transverse plane by using the following parameters: TR/TE, 407/10; bandwidth, 20.83 kHz; matrix size, 256 × 256; field of view (FOV), 22 × 22 cm; number of sections, 20; section thickness, 5 mm; and gap, 1 mm. T2-weighted fast spin-echo images were acquired with the following parameters: TR/TE, 4555/125; bandwidth, 20.83 kHz; matrix size, 256 × 256; FOV, 22 × 22 cm; number of sections, 20; section thickness, 5 mm; and gap, 1 mm.

Diffusion-weighted imaging was performed by using a diffusion-weighted single echo-planar MR imaging sequence. During the MR studies, the two experienced radiologists cited above evaluated the quality of diffusion-weighted images and selected by consensus those images for further analysis that had a minimum of distortion from susceptibility artifacts and ghosting. We selected b values of 0 and 1000 s/mm^2 for calculation of ADCs in this study. Diffusion-weighted images were obtained over 43 seconds. Diffusion-weighted imaging was performed with the following parameters: TR/TE, 7216/122.8; flip angle, 90°; FOV, 24 × 24 cm; and matrix size, 128 × 128 mm. Between 20 and 24 axial sections were obtained, with a section thickness of 5 mm and an intersection gap of 2.5 mm.

The reconstructed magnitude images were transferred from the MR system to an independent workstation for the calculation of the trace images and ADC values.

Mean ADC values for each group ($\times 10^{-3}$)

	A	B	C	D	E	F	G	H
Sentrium semiovale	0.733	0.738	0.734	0.748	0.745	0.764	0.735	0.770
Frontal white matter	0.814	0.806	0.805	0.806	0.795	0.819	0.789	0.818
Caudate nucleus	0.766	0.754	0.766	0.764	0.782	0.758	0.789	0.764
Putamen	0.763	0.735	0.762	0.743	0.777	0.765	0.764	0.769
Thalamus vm	0.738	0.709	0.745	0.738	0.779	0.761	0.768	0.764
Substantia nigra	0.807	0.750	0.781	0.769	0.767	0.737	0.776	0.754
Red nucleus	0.755	0.747	0.755	0.759	0.689	0.758	0.724	0.758
Pons	0.712	0.735	0.704	0.719	0.702	0.716	0.727	0.723

Note.—A, ADC value obtained with small region of interest (ROI) size (22 ± 5 mm^2) with observer 1 on the right hemisphere; B, ADC value obtained with small ROI size (22 ± 5 mm^2) with observer 2 on the right hemisphere; C, ADC value obtained with larger ROI size (62 ± 6 mm^2) with observer 1 on the right hemisphere; D, ADC value obtained with larger ROI size (62 ± 6 mm^2) with observer 2 on the right hemisphere; E, ADC value obtained with small ROI size (22 ± 5 mm^2) with observer 1 on the left hemisphere; F, ADC value obtained with small ROI size (22 ± 5 mm^2) with observer 2 on the left hemisphere; G, ADC value obtained with larger ROI size (62 ± 6 mm^2) with observer 1 on the left hemisphere; H, ADC value obtained with larger ROI size (62 ± 6 mm^2) with observer 2 on the left hemisphere.

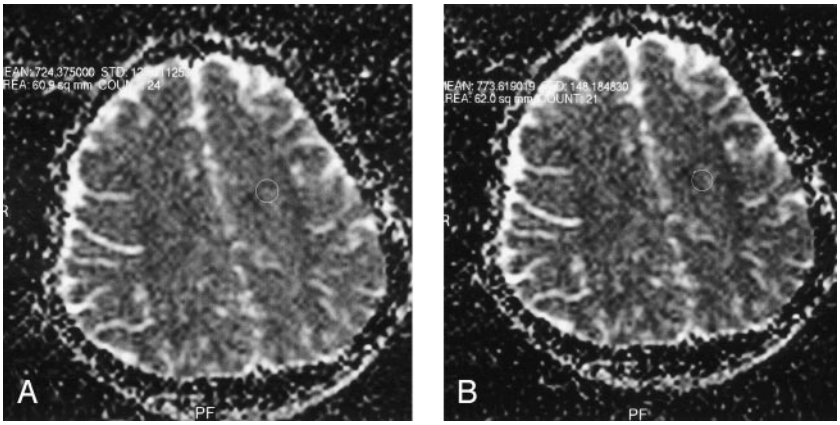

FIG 1. ADC values obtained from the sentrium semiovale.
A, Observer 1.
B, Observer 2.

To ensure accurate localization and consistency of measurements, the two blinded radiologists independently placed ROI areas on the right and left side of the brain in different characteristic gray and white matter structures (centrum semiovale, frontal white matter, nucleus caudatus, putamen, thalamus, substantia nigra, red nucleus, and pons) on the images obtained with a b value of 1000 s/mm^2. At each prespecified site, two ADC values were obtained by using two different-sized ROI areas (smaller ROI within larger ROI).

ADC values were recorded from the different sites of the brain mentioned above for each hemisphere. The two radiologists independently performed this procedure. Each measurement was repeated by using two ROI areas, one inside the other (average areas of regions of interest were 22 ± 5 mm^2 and 62 ± 6 mm^2, respectively).

For statistical analysis, we first compared ADC values for each observer from each measurement site with a paired *t* test. Later, for comparison of different ROI areas, ADC values obtained with different ROI areas were compared with a paired *t* test. The significance level was set $P < .05$.

Results

Our study population consisted of 27 subjects with an age range of 2 months to 62 years and a mean age of 43.4 ± 17 years. This group included 14 male and 13 female subjects. Imaging examinations of the patients showed no abnormalities.

Mean ADC values for each group is demonstrated in the Table.

ADC values obtained from the left and right side for each measurement site did not differ statistically ($P > .05$).

Using the paired *t* test, we found a statistically significant interobserver difference in ADC values obtained from the centrum semiovale, frontal white matter, pons, substantia nigra, and red nucleus ($P = .031$; $P = .019$; $P = .044$; $P = .028$; $P = .001$ respectively). ADC values among different-sized ROI areas approached statistical significance only in the substantia nigra, red nucleus, and pons ($P = .016$; $P = .002$; $P = .037$ respectively) (Figs 1–3).

Discussion

Diffusion-weighted imaging is being used with increasing frequency in many clinical and experimental circumstances. Systems equipped with high-speed gradients allow performance of diffusion imaging in less then 1 minute; results can be immediately displayed without the need for off-line processing. Because of this speed, ease of performance, and utility in the detection of pathologic processes, particularly in the detection of acute infarction, diffusion-weighted imaging has become a routine component of brain MR imaging protocols at many institutions (2).

Diffusion-weighted imaging has been successfully used not only in the central nervous system for diagnosis of early cerebral ischemia, multiple sclerosis,

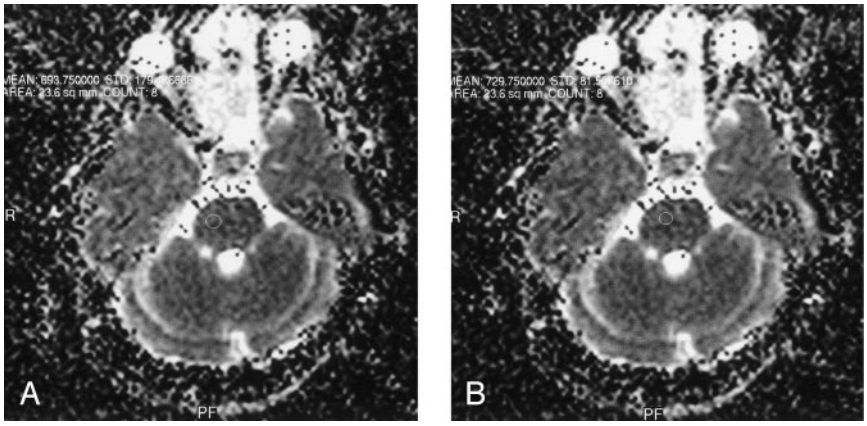

FIG 2. ADC values obtained in the pons.
A, Observer 1.
B, Observer 2.

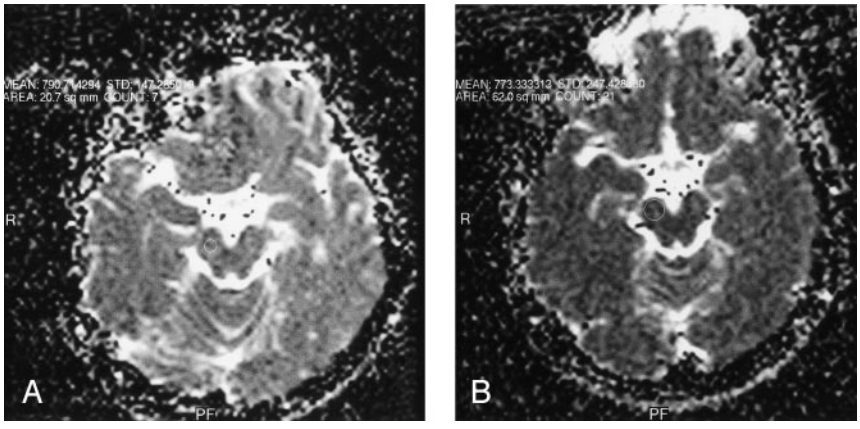

FIG 3. ADC values obtained in the substantia nigra.
A, ADC value obtained by observer 1 from the substantia nigra with a small region of interest size.
B, ADC value obtained by observer 1 from the substantia nigra with a larger region of interest size.

gliomas, and brain abscess and to differentiate between arachnoid cysts and epidermoid cysts and other diseases (3–9), but also has been used in regions outside the central nervous system for differentiation between benign and malignant lesions in the liver and bone marrow (10, 11). Diffusion-weighted imaging is also used for identification of different cystic lesions in abdominal organs (12).

Diffusion-weighted imaging is sensitive to alterations in the translational motion of water molecules in the region of brain studied and has had a significant impact on clinical imaging. Random motion of water molecules is relatively free in homogeneous, fluid-containing structures. This type of water diffusion is called isotropic diffusion. On the other hand, in tissue such as brain parenchyma, water motion is restricted by the presence of cellular structures that provide barriers to free diffusion (13). This restriction may be more in one direction than in another (eg, around axons). This type of water diffusion is called anisotropic diffusion. Because water protons in each portion of tissue contribute differently to overall diffusion in the tissue, any architectural changes, including the change in the proportion of extracellular water protons, will alter the ADC measured in the tissue (12).

ADC values are known to be rotationally invariant measurements of the amount of total diffusion within a tissue (13). Mean ADC values of benign solid lesions have been found to be significantly higher than those of malignant tumors, and ADC values have also been correlated with degree of tumor cellularity (10, 14, 15). It is also established that reversible ADC changes in humans are rare but have been found in cases of transient ischemic attack in which imaging is performed within 4 hours of symptom onset, status epilepticus, venous infarction associated with seizures, and hemiplegic migraine (16). ADC values have also been found to be significantly higher in the globus pallidus of 3,4-methylenedioxymethamphetamine ("ecstasy") users (17). Some investigators have found that increased ADC values correlate with advancing age (3, 18, 19). Therefore, application of ADC values gains importance, because in many diseases these measurements can be used not only to support diagnosis but also treatment and follow-up.

ADC values can be calculated either automatically by use of generated ADC maps with ROI or pixellens evaluation or from the Stejskal-Tanner (13) ROI measurements. These methods depend on correct identification of the measured structure by the operator, and ROI measurements make use of only those pixels in the ROI area, whereas distribution analysis uses all pixels. Alternatively, multiple ROI measurements are limited for several reasons. Choice of location and number and size of ROI areas are operator dependent (3). This can lead to site-selection bias, which limits the reproducibility of results. ROI areas may include heterogeneous tissue (eg, white matter and CSF), and measurements of diffusion may fail to reveal changes occurring in brain parenchyma. As

ROI volume increases, many fibers may intersect, resulting in ADC variance (2).

In addition, several applications of diffusion-weighted imaging would benefit significantly from the use of smaller voxels if an appropriate signal-to-noise ratio could be obtained in a clinically acceptable measurement time. In the typical diffusion-tensor MR imaging experiment, an ROI volume of $2 \times 2 \times 5$ mm^3 is used, so several fibers may intersect within one voxel, resulting in unwanted partial-volume effects (20).

In our study, we found a statistically significant difference of ADC values between two blinded observers at the centrum semiovale, frontal white matter, pons, substantia nigra, and red nucleus. Also, variation of ROI sizes caused significant differences at pons, substantia nigra, and red nucleus. The close relationship of these sites to CSF and fibers intersecting as ROI volume increases might be the possible explanation for the statistical difference.

Conclusion

Variation of ADC values obtained by two observers was statistically significant. The relationship of selected sites to CSF, variation in ROI localization between the observers, and an increasing number of fibers intersecting as ROI volume increases might be the possible explanation. Despite that observers were careful about placement of ROI areas, low signal-to-noise ratios of diffusion-weighted images might lead to misinterpretation. Thus, ADC can be unreliable for use in assessing brain disease in certain areas.

Acknowledgments

The authors acknowledge the help of Osman Caglayan from the Department of Biochemistry for statistical analysis and Yilmaz Karadeniz for his help. Without their help, this project could not have been completed.

References

1. Sorensen AG, Copen WA, Davis TL, et al. **Acute cerebral ischemia: detection of changes in water diffusion anisotropy by using MR imaging.** *Radiology* 0000:212:785–792
2. Wang J, Takashima S, Takayama F, et al. **Head and neck lesions: characterization with diffusion-weighted echo-planar imaging.** *Radiology* 2001;220:621–630
3. Chun T, Filippi CC, Zimmerman, Ulug A. **Diffusion changes in the aging human brain.** *AJNR Am J Neuroradiol* 2000;21:1078–1083
4. Moseley ME, Kucharczyk J, Mintorovitch J, et al. **Diffusion-weighted MR imaging of acute stroke:correaltion with T2–weighted and magnetic susceptibility-enhanced MR imaging in cats.** *AJNR Am J Neuroradiol* 1990;11:423–429
5. Sorensen AG, Buananno FS, Gonzalaz RG, et al. **Hyperacute stroke: evaulation with combined multisection diffusion-weighted and hemodynamically weighted echo-planar imaging. Radiology** 1996;199:391–401
6. Larson HBW, Thomsen C, Frederiksen J, et al. **In vivo magnetic resonance diffusion measurement in the brain of patients with multiple sclerosis.** *Magn Reson Imaging* 1993;10:712.
7. Brunberg JA, Chenevert TL, McKeever PE, et al. **In vivo MR determination of water diffusion coeeficients and diffusion anisotropy: correlation with structural alteration in gliomas of creberal hemispheres.** *AJNR Am J Neuroradiol* 1995;16:361–371
8. Noguchi K, Watanabe N, Nagayoshi T, et al. **Role of diffusion weighted echo-planar MRI in distinguishing between brain abscess and tumour: a preliminary report.** *Neuroradiology* 1999;41:171–174
9. Tsuruda SJ, Chew MW, Moseley EM, Norman D. **Diffusion-weighted MR imaging of the brain:value of differentating between extraaxial cysts and epidermoid tumors.** *AJNR AM J Neuroradiol* 1990;11.925–931.
10. Kono K, Inoue Y, Nakayama K, et al. **The role of diffusion-weighted imaging in patients with brain tumors.** *AJNR Am J Neuroradiol* 2001;22:1081–1088.
11. Namimoto T, Yamashita Y, Sumi S, et al. **Focal liver masses: characterization with diffusion-weighted echo-planar MR imaging.** *Radiology* 1997;204:739–744
12. Baur A, Stabler A, Brüning R, et al. **Diffusion-weighted MR imaging of bone marrow: differentation of benign versusu pathologic compression fractures.** *Radiology* 1998;207:349–356
13. Sener RN. **Diffusion MRI: apparent diffusion coefficient (ADC) values in the normal brain and a classification of brain disorders based on ADC values.** *Comput Med Imaging Graph* 2001;25:299–326
14. Castillo M, Smith JK, Kwock L, Wilber K. **Apparent diffusion coefficients in the evaulation of high-grade cerebral gliomas.** *AJNR Am J Neuroradiol* 2001;22:60–64
15. Hakyemez B, Parlak M. **Characterization of intracranial cystic and necrotic lesions with FLAIR and diffusion-weighted EPI MRI.** *Turk J Diagn Intervent Radiol* 2002;8:19–26
16. Grant PE, He HJ, Halpern E, et al. **Frequency and clinical context of decreased apparent diffusion coefficient reversal in the human brain.** *Radiology* 2001;221:43–50
17. Reneman L, Majoie CBLM, Habraken JBA, Heeten GJD. **Effect of ecstasy (MDMA) on the brain in abstinent users: initial observations with diffusion and perfusion MR imaging.** *Radiology* 2001; 220:611–617
18. Engelter ST, Provenzale JM, Petrella JR, et al. **The effect of aging on apparent diffusion coefficient of normal appearing white matter.** *AJR Am J Roentgenol* 2000;175:425–430
19. Nusbaum AO, Tang CY, Buchsbaum MS. Regional and global changes in cerebral diffusion with normal aging. *AJNR Am J Neuroradiol* 2001;22:136–142
20. Hunsche S, Moseley M, Stoeter P, et al. Diffusion-tensor MR imaging at 1.5 and 3.0 T: initial observations. *Radiology* 2001;221: 550–556